Chemistry & Biology
Article

Development of an IL-6 Inhibitor Based on the Functional Analysis of Murine IL-6Rα[1]

Monique Y. Wiesinger,[1] Serge Haan,[2] Stefan Wüller,[1,3] Maria-Elisabeth Kauffmann,[1] Tobias Recker,[1] Andrea Küster,[1] Peter C. Heinrich,[4] and Gerhard Müller-Newen[1,*]
[1]Institut für Biochemie, Universitätsklinikum RWTH Aachen, 52074 Aachen, Germany
[2]Life Science Research Unit, Faculté des Sciences, de la Technologie et de la Communication, Université du Luxembourg, 1511 Luxembourg, Luxembourg
[3]Klinik für Kinder und Jugendmedizin,Universitätsklinikum RWTH Aachen, 52074 Aachen, Germany
[4]Institut für Biochemie und Molekularbiologie, ZBMZ, Universität Freiburg, 79104 Freiburg, Germany
*Correspondence: mueller-newen@rwth-aachen.de
DOI 10.1016/j.chembiol.2009.06.010

SUMMARY

Dysregulated cytokine production contributes to inflammatory and proliferative diseases. Therefore, inhibition of proinflammatory mediators such as TNF, IL-1, and IL-6 is of great clinical relevance. Actual strategies are aimed at preventing receptor activation through sequestration of the ligand. Here we describe the development of an inhibitor of murine IL-6 based on fused receptor fragments. Molecular modeling-guided analysis of the murine IL-6Rα revealed that mutations in the Ig-like domain D1 severely affect protein function, although D1 is not directly involved in the ligand-binding interface. The resulting single chain IL-6 inhibitor (mIL-6-RFP) consisting of domains D1–D3 of mgp130, a flexible linker, and domains D1–D3 of mIL-6Rα is a highly potent and specific IL-6 inhibitor. mIL-6-RFP will permit further characterization of the role of IL-6 in various disease models and could ultimately lead to anti-IL-6 therapy.

INTRODUCTION

Elevated IL-6 levels have been observed in a variety of inflammatory and autoimmune diseases such as rheumatoid arthritis, Crohn's disease, and lupus erythematosus (Ishihara and Hirano, 2002). Recently it has been described that besides other cytokines IL-6 plays an important role in the differentiation of Th17 cells (Bettelli et al., 2008). This finding provides a rational explanation for a causative role of IL-6 in autoimmune diseases (Serada et al., 2008). The proinflammatory activities of IL-6 might act as a molecular link to inflammation-related cancers (Naugler and Karin, 2008). Thus, IL-6 has emerged as an important target molecule in the therapy of human diseases.

The use of soluble receptors is a promising approach for the generation of highly potent and specific cytokine inhibitors (Goldenberg, 1999). IL-6 is a pleiotropic cytokine that binds to a receptor consisting of two subunits: the IL-6-specific nonsignaling receptor subunit IL-6Rα that is found only on a restricted number of cell types and the ubiquitously expressed signal-transducing receptor subunit gp130 (Müller-Newen, 2003). Gp130 mediates activation of the Jak/STAT signaling pathway (Heinrich et al., 2003), which leads to the expression of well defined STAT3 target genes including the acute phase proteins, Bcl-2, and VEGF (Sepulveda et al., 2007; Wegenka et al., 1994; Wei et al., 2003).

Besides the membrane-bound IL-6Rα, a soluble form exists (sIL-6Rα) that also binds IL-6 and transfers IL-6 responsiveness to cells lacking membrane-bound IL-6Rα in a process termed trans-signaling (Scheller et al., 2006). Inhibition of IL-6 by the use of soluble receptors is challenging because of the agonistic property of sIL-6Rα. However, complexes of IL-6 and sIL-6Rα can be neutralized by a soluble form of gp130 (sgp130) (Müller-Newen et al., 1998). Both sIL-6Rα and sgp130 are present in human body fluids. These naturally occurring soluble receptors are generated by proteolytic processing of membrane-bound receptors or translation of an alternatively spliced mRNA (Levine, 2004).

Boulanger et al. (2003) crystallized the IL-6 receptor complex consisting of human IL-6 bound to soluble fragments of human IL-6Rα and human gp130. The structure reveals a hexameric complex with a $(IL\text{-}6/IL\text{-}6R\alpha/gp130)_2$ stoichiometry. Receptor binding occurs through three conserved epitopes of IL-6 (sites I, II, and III) (Figure 1A). IL-6 binds with its site I to domains 2 and 3 (D2 and D3) of IL-6Rα. D2 and D3 constitute the so called cytokine binding module (CBM) that dominates this interaction. Only the heterodimeric complex of IL-6 and IL-6Rα is a substrate for the engagement of gp130 through site II and III interactions (Figure 1A). Site II is a composite epitope consisting of contacts between IL-6 and the domains D2 and D3 of gp130 (site IIa) and between amino acids of IL-6Rα and gp130 (site IIb). Through a subsequent interaction involving site III of the cytokine and the Ig-like domain (D1) of gp130 the high affinity signaling complex is formed. The site III interaction can also be subdivided in the interaction between IL-6 and D1 of gp130 (site IIIa) and IL-6Rα and gp130 (site IIIb) (Boulanger et al., 2003).

We have recently established a fusion protein of the ligand binding domains of human IL-6Rα (domains D2 and D3) and human gp130 (domains D1, D2, and D3) that acts as a highly potent and specific inhibitor for human IL-6 (Ancey et al., 2003; Metz et al., 2007). Because murine IL-6 does not bind to human IL-6Rα (Grötzinger et al., 1997) this inhibitor is not suited for an application in animal models. Therefore, we set out to generate a receptor fusion protein for the inhibition of murine IL-6 consisting of the respective murine receptor proteins. Interestingly,

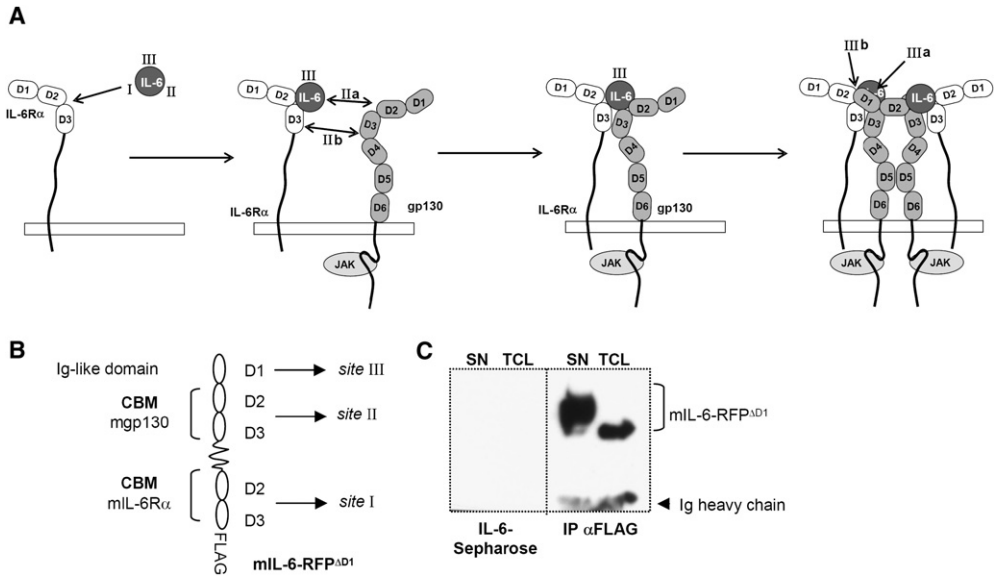

Figure 1. A Murine IL-6 Receptor Fusion Protein (mIL-6RFP$^{\Delta D1}$) Built Up in Analogy to the Human IL-6 Receptor Fusion Protein Does Not Bind IL-6

(A) Assembling of the IL-6 receptor complex according to Boulanger et al. (2003). Interleukin-6 binds the receptor subunits with three conserved sites (sites I, II, and III). The interaction of site I with the nonsignaling IL-6Rα chain is dominated by domains D2 and D3 of the receptor. The binary IL-6/IL-6Rα complex recruits gp130 through site IIa and site IIb interactions. Two of these trimeric complexes dimerize via site IIIa and site IIIb interactions, resulting in the formation of the final hexameric signaling complex.

(B) A murine receptor fusion protein was constructed that lacks D1 of IL-6Rα in accordance with the formerly described human IL-6-RFP (Ancey et al., 2003). mIL-6RFP$^{\Delta D1}$ consists of D1–D3 of murine gp130 followed by a 41 amino acid flexible polypeptide linker, domains D2 and D3 of murine IL-6Rα, and a C-terminal FLAG tag. D2 and D3 of each receptor constitute the respective CBM. Interactions with the sites I, II, and III of IL-6 are indicated by arrows.

(C) IL-6-binding assay. Supernatants (SN) and total cellular lysates (TCL) of COS-7 cells stably transfected with an expression vector encoding mIL-6RFP$^{\Delta D1}$ were subjected to precipitation with IL-6-Sepharose or immunoprecipitation with a FLAG antibody. Precipitated proteins were analyzed by western blot analysis using the FLAG antibody.

a murine receptor fusion protein constructed in analogy to the human receptor fusion protein does not bind IL-6. By molecular modeling-guided mutagenesis we found that the Ig-like domain (D1) of the murine IL-6Rα is required for receptor surface expression and IL-6 binding. Based on these findings we present a novel receptor fusion protein consisting of domains D1, D2, and D3 of murine IL-6Rα fused to domains D1, D2, and D3 of murine gp130. This fusion protein acts as a highly potent inhibitor for murine, rat, and human IL-6.

RESULTS

A Murine IL-6-RFP Lacking the Ig-like Domain D1 of mIL-6Rα Does Not Bind IL-6

In the present study we aimed at generating a potent and cytokine-specific inhibitor of murine IL-6 in analogy to our previously described fusion protein approach for the inhibition of human IL-6 (Ancey et al., 2003). According to the composition of the human receptor fusion protein hIL-6-RFP, we first generated a fusion protein consisting of domains D1, D2, and D3 of murine gp130 (comprising the Ig-like domain and the CBM) and domains D2 and D3 of murine IL-6Rα (comprising the CBM). The receptor domains were fused using a polypeptide linker of 41 amino acids and a C-terminal FLAG tag was added for detection purposes (Figure 1B). According to this concept, domain D1 of IL-6Rα was not included in the fusion protein (mIL-6-RFP$^{\Delta D1}$). We previously showed that the corresponding human receptor fusion protein hIL-6-RFP binds IL-6 with high affinity and inhibits IL-6 responses (Metz et al., 2007). For a first functional investigation, mIL-6-RFP$^{\Delta D1}$ was stably expressed in COS-7 cells. Supernatants of cells were collected and cellular lysates were prepared. Ligand binding of mIL-6-RFP$^{\Delta D1}$ was analyzed by precipitation with immobilized IL-6. In parallel, the fusion protein was precipitated both from supernatant and cellular lysates with a FLAG antibody to prove expression of the recombinant protein. Figure 1C shows that the murine receptor fusion protein mIL-6-RFP$^{\Delta D1}$ lacking domain D1 of mIL-6Rα does not bind to immobilized IL-6 although it is present in both supernatant and lysate. Accordingly, mIL-6RFP$^{\Delta D1}$ does not inhibit IL-6 bioactivity (data not shown).

Structural Comparison of Murine and Human IL-6Rα

In order to investigate whether different structural requirements for IL-6 binding by murine and human IL-6-RFP may contribute to the loss of ligand-binding capacity, we generated model structures of murine gp130 and murine IL-6Rα based on the solved crystal structures of the human proteins (Boulanger et al., 2003; Varghese et al., 2002). The most striking differences were observed for IL-6Rα. Figure 2A shows a section of the alignment of IL-6Rα sequences of different origin and illustrates the high degree of homology between different species. The most prominent differences between the solved crystal structure

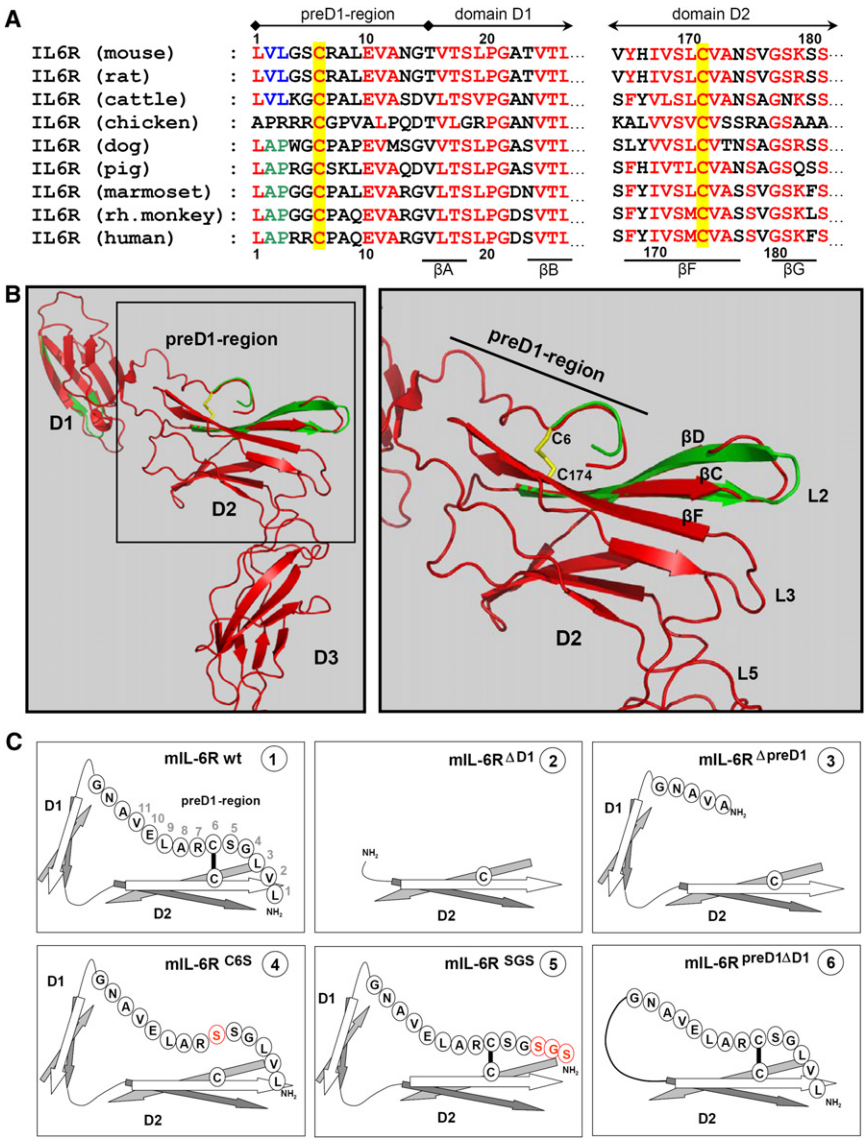

Figure 2. Structural Analysis of Murine IL-6Rα

(A) Sections (preD1 region, parts of D1 and D2) of the sequence alignment of IL-6Rα from different species. Highly conserved residues are depicted in red. The hydrophobic Val-Leu and Ala-Pro motifs conserved in some of the species are represented in blue and green, respectively. Cysteine residues involved in the disulfide bond involving Cys6 are highlighted in yellow. Secondary structure elements for human IL-6Rα (Varghese et al., 2002) as well as amino acid numbers for human and murine IL-6Rα are given.

(B) Overlay of the ribbon representations of the solved structure (Varghese et al., 2002) of human IL-6Rα (red ribbon, domains D1 to D3; Brookhaven data bank entry code 1N26) and our model structure of the corresponding domains of murine IL-6Rα (green ribbon). The disulfide bond involving Cys6 and Cys174 (human IL-6Rα) is represented as a stick model. The program PyMOL was used for representation of the structures.

(C) Schematic representation of the generated mutants of murine IL-6Rα. Some of the β strands in domains D1 and D2 are indicated by arrows. The amino acids of the preD1 region as well as the disulfide bridge are shown. Point mutations are highlighted in red.

of human IL-6Rα and the model structure of murine IL-6Rα become apparent in the overlay of hIL-6Rα (red ribbon) and mIL-6Rα (green ribbon) represented in Figure 2B. These predicted structural differences are located in the region preceding domain D1 (preD1 region) as well as in domains D1 and D2. The preD1 region is part of a remarkable structural feature of the IL-6Rα: it folds back to domain D2, where it is covalently fixed by a disulfide bond between Cys6 in the preD1 region and Cys174 in D2 (Cys171 in the murine receptor) resulting in a precise positioning of the N-terminal amino acids. Strikingly, the N-terminal amino acids and the region within domain D2 that is contacted by these amino acids differ in the human and murine proteins. The presence of larger hydrophobic amino acid side chains for the residues at the positions 2 and 3 in murine IL-6Rα (Val2 and Leu3, Figures 2A and 2C [1]) could indicate a stronger interaction with the surrounding amino acids of domain D2. In this region domain D2 of the murine receptor is characterized by an extension of the region encompassing the strands βD and βC as well as the connecting loop L2. In the human system, this loop contributes to IL-6 binding, although to a lesser extent than the loops L3 and L5 located in domains D2 and D3, respectively. It is thus conceivable that the hydrophobic N-terminal amino acids of the preD1 region contribute to IL-6 binding by orienting or stabilizing the region around the beta strands βD and βC in domain D2.

Based on this structural analysis we investigated the contribution of N-terminal amino acids and the disulfide bond to receptor function. For this purpose we generated several point and deletion mutants of the murine IL-6Rα. An IL-6Rα construct lacking both the preD1 region as well as domain D1 (mIL-6R$^{\Delta D1}$; Figure 2C [2]) was generated in order to verify the results shown in Figure 1C. Furthermore, the first 11 amino acids of the preD1 region were deleted to study its potential importance for IL-6 binding (mIL-6R$^{\Delta preD1}$; Figure 2C [3]). In order to evaluate the importance of the cysteine bridge between the preD1 region and domain D2, we mutated Cys6 to Ser to prevent the formation of the disulfide bond (mIL-6R^{C6S}; Figure 2C [4]). To assess the importance of the N-terminal part of the preD1 region, the first three amino acids (Leu1, Val2, and Leu3) were replaced by a Ser-Gly-Ser motif (mIL-6R^{SGS}; Figure 2C [5]). Finally, the core domain D1 was deleted by connecting the preD1 region to domain D2 (mIL-6R$^{preD1\Delta D1}$; Figure 2C [6]). As can be seen in Figure 2B, the C terminus of the preD1 region is in close proximity to the N terminus of domain D2 so that the two regions can easily be linked.

Functional Importance of the First Domain (D1) of the Murine IL-6 Receptor α Subunit

Murine IL-6 does not bind to human IL-6Rα (Grötzinger et al., 1997). Therefore, the human HepG2 cell line was used to study the murine IL-6Rα mutants without background of endogenous receptors. HepG2 cells were stably transfected with expression vectors encoding wild-type and mutant murine IL-6Rα tagged with the yellow fluorescent protein (YFP) at their C termini. Cell surface expression of the receptor proteins was analyzed by flow cytometry (Figure 3A). Only wild-type and the SGS mutant are expressed at the cell surface, all the other mutants were not detectable. This finding was corroborated by confocal laser-scanning microscopy of living cells (Figure 3B). Only mIL-6Rα wild-type and the SGS mutant colocalizes with the trypan blue staining that marks the plasma membrane. The other mutants remain in intracellular reticular structures. Thus, domain D1 and the disulfide bond between the preD1 region and D2 are required for cell surface expression of mIL-6Rα. The preD1 region in the absence of D1 is not sufficient to warrant cell surface expression (Figure 3, last panels).

Next we investigated whether the SGS mutation at the N terminus of mIL-6Rα interferes with the bioactivity of the receptor in terms of IL-6-mediated receptor activation. DNA binding of activated STATs and induction of a STAT3-specific reporter gene were analyzed. HepG2 cells stably transfected with IL-6Rα wild-type or the SGS mutant were first analyzed by flow cytometry (Figure 4A) before they were used for the experiments depicted in Figures 4B and 4C. Quantitative analysis of the flow cytometry data revealed a somewhat higher cell surface expression of the SGS mutant compared to wild-type protein. These cells were stimulated for a short time period (20 min) with different concentrations of mIL-6 (25 pg/ml up to 2.5 ng/ml). Nuclear extracts were prepared and DNA-bound STAT proteins were analyzed by electrophoretic mobility shift assay (EMSA). Equal amounts of nuclear protein of both cell lines were incubated with a P^{32}-labeled oligonucleotide containing a STAT binding site. The upper part of Figure 4B shows shifted bands of DNA-bound STAT1 and STAT3 species from both cell lines. STAT3 homodimers represent the most prominent dimer species after mIL-6 stimulation. The corresponding band is weaker in cells expressing the SGS mutant compared to wild-type protein. Similarly, the proportion of STAT1/3 heterodimers and STAT1/1 homodimers, which preferentially form at higher cytokine concentrations, differs considerably between wild-type receptor and mutant as is evident from the quantitative evaluation of the autoradiography (diagrams in Figure 4B).

To further determine the biological relevance of the distinct differences in the activation patterns for both receptors, transcriptional activity of activated STAT proteins was analyzed in both cell lines. Cells were transfected with a STAT3-inducible reporter gene construct containing the rat α2M promoter and a control plasmid. Cells were stimulated with mIL-6 (2.5, 5, and 10 ng/ml) for 18 hr and luciferase activity was measured. Figure 4C shows a considerably reduced reporter gene induction in cells expressing the SGS mutant compared to wild-type. The effect is most prominent at low cytokine concentrations. Taken together, the mutation of N-terminal amino acids diminishes the bioactivity of the murine IL-6Rα.

A Murine IL-6 Receptor Fusion Protein Comprising D1 of IL-6Rα (mIL-6-RFP) Binds IL-6

All of the mIL-6Rα mutants lacking the N-terminal Ig-like domain D1 or at least the disulfide bond between the preD1 region and D2 were not expressed at the cell surface and thus not accessible for functional binding assays. Therefore, we decided to analyze IL-6 binding of these mutants in the context of a receptor fusion protein with domains D1–D3 of murine gp130. All receptor fusion proteins were equipped with a V5 epitope tag at their C termini and stably expressed in HEK293 cells. Figure 5 shows the analysis of protein expression in cellular lysates and supernatants by precipitation with a V5 antibody. Ligand binding was analyzed by precipitation with immobilized IL-6. Again, all the mutants lacking domain D1 or the disulfide bond between the preD1 region and D2 of mIL-6Rα were weakly expressed, indicating a prominent role of these structural features for processing, folding, and secretion of the protein. Most interestingly, the expressed mutants are not precipitated with immobilized IL-6, indicating impaired ligand binding (Figure 5, lanes 2, 14, 18, and 22).

The fusion protein derived from mIL-6Rα wild-type is most strongly expressed. In the cellular lysate (Figure 5, lane 11), besides the mature form that corresponds to the band in the supernatant (Figure 5, lane 12), a non-terminally processed form of lower molecular mass is visible. Both forms are precipitated with IL-6-Sepharose (Figure 5, lanes 9 and 10), indicating that glycosylation of the fusion protein is not required for ligand binding. Comparison of the precipitation of the fusion proteins derived from mIL-6Rα wild-type and the SGS mutant reveals that the SGS mutation leads to a decrease in IL-6 binding (Figure 5, compare lanes 6, 8, 10, and 12). This finding is in line with the reduced bioactivity of the SGS mutant (Figure 4). The fusion protein consisting of D1, D2, and D3 of mgp130 and D1 (including the preD1 domain), D2, and D3 of mIL-6Rα termed mIL-6-RFP was further characterized.

The complex of mIL-6-RFP and IL-6 was analyzed by blue native PAGE. The native gel loaded with different amounts of mIL-6-RFP and YFP-hIL-6 was scanned with a fluorescence scanner. The complex of YFP-hIL-6 (50 kDa) and mIL-6-RFP (100 kDa) has an apparent molecular mass of 600 kDa (Figure 5B, left panel) that corresponds to four molecules of each of YFP-hIL-6 and mIL-6-RFP in the complex. To verify this observation a similar experiment was performed with mIL-6 (20 kDa). This protein is non-fluorescent and therefore was detected by western blotting (Figure 5B, right panel). The apparent molecular mass of the complex corresponds to about 500 kDa, again arguing for a complex of $(mIL\text{-}6)_4(mIL\text{-}6\text{-}RFP)_4$ stoichiometry. Non-bound IL-6 is not detectable in the native gel or western blot due to its low molecular mass.

mIL-6-RFP Is a Potent Inhibitor for Murine, Rat, and Human IL-6

Human IL-6 acts on human, murine, and rat cells, whereas murine IL-6 only acts on cells expressing murine IL-6Rα. We therefore tested whether mIL-6-RFP is able to inhibit IL-6 of different species. Human HepG2 hepatoma, murine B9 hybridoma, and rat Fao hepatoma cells were stimulated for 20 min with human, murine, and rat IL-6, respectively, in the presence of supernatants from HEK293 cells stably expressing mIL-6-RFP or control

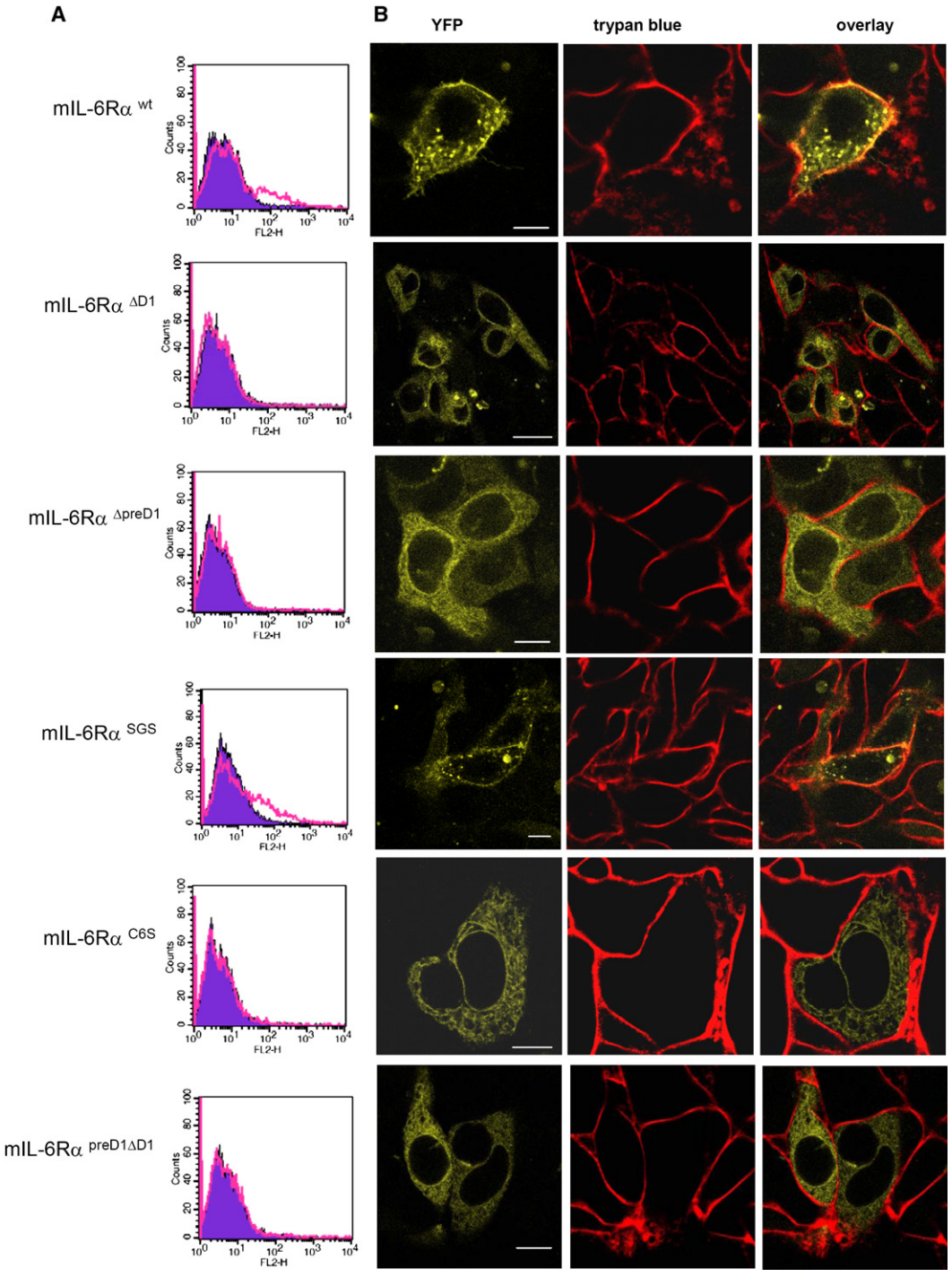

Figure 3. Subcellular Localization of IL-6Rα Mutants

(A) HepG2 cells were stably transfected with the mutants of murine IL-6Rα (Figure 2C) fused to YFP at their C termini. Cell surface expression was analyzed by flow cytometry using an mIL-6Rα antibody and a phycoerythrin-conjugated secondary antibody (red histograms). The isotype controls are shown as blue histograms. (B) Living HepG2 cells stably transfected with the IL-6Rα-YFP constructs were analyzed by confocal microscopy. The membrane was stained with trypan blue. YFP fluorescence is shown in yellow, trypan blue fluorescence in red. Scale bars represent 10 μm.

supernatants from mock transfected cells. The concentration of the fusion protein was determined by ELISA. Cellular lysates were prepared and tyrosine phosphorylation of STAT3 was analyzed by western blotting. Equal loading was verified by staining of total STAT3. Figure 6A shows that mIL-6-RFP inhibits the bioactivity of IL-6 from all three species with comparable efficacy.

Next the cytokine-specificity of mIL-6-RFP was analyzed. IL-11, OSM, and CNTF, which share the signal transducing

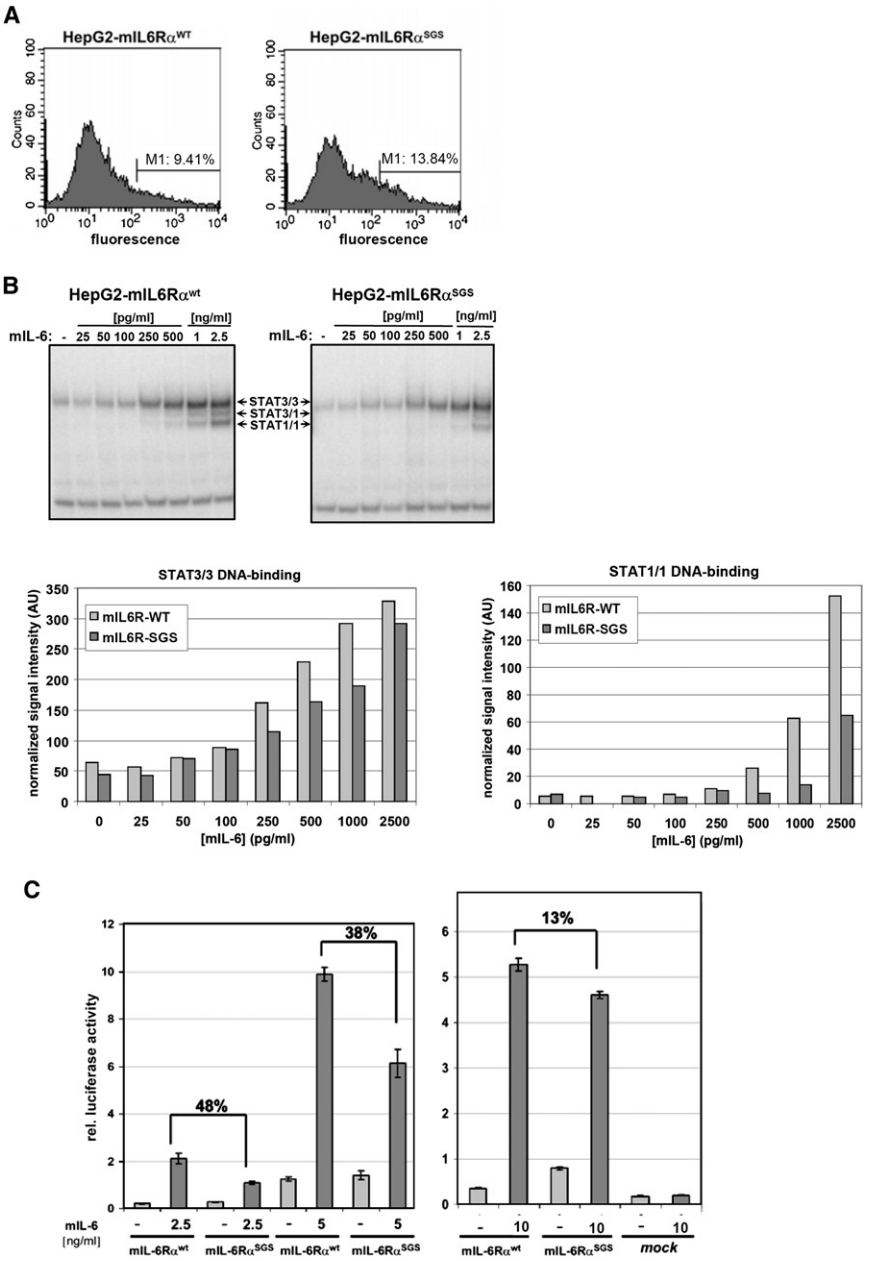

Figure 4. Activity of the SGS Mutant Compared to IL-6Rα Wild-Type

(A) HepG2 cells expressing mIL-6Rα-YFP wild-type or the mIL-6Rα^{SGS}-YFP mutant were analyzed by flow cytometry for receptor surface expression as described in Figure 3A. The portion of highly fluorescent cells beyond the marker M1 is indicated in the histograms.

(B) After FACS analysis the stably transfected HepG2 cells were stimulated with different amounts of mIL-6 for 20 min as indicated. Nuclear extracts were prepared and incubated with a [^{32}P]-labeled SIEm67 probe (Wagner et al., 1990). STAT DNA binding was analyzed by an EMSA. DNA-bound STAT species were visualized by autoradiography. All samples were run on the same gel. The radioactivity was quantified with a PhosphoImager. The intensities of the STAT bands were normalized with the intensities of the nonspecific bands at the bottom of the gel. The values are depicted as bar charts.

(C) Stably transfected HepG2 cells were transiently transfected with a reporter gene plasmid encoding firefly luciferase under control of an IL-6-responsive α2M promoter and a constitutively active promotor construct encoding renilla luciferase. Twelve hours after transfection cells were stimulated for 16 hr with mIL-6 at different concentrations as indicated. Subsequently cells were lysed and luciferase activities were measured. The diagrams show the normalized reporter gene induction from cells transfected with IL-6Rα wild-type or the SGS mutant. The percent reduction of the response evoked by the SGS mutant compared to the wild-type response is indicated. Standard deviations are shown for a triplicate experiment.

receptor subunit gp130, belong to the cytokines most closely related to IL-6. HepG2 cells were stimulated with IL-6, IL-11, and OSM for 20 min in the presence of supernatants containing mIL-6-RFP. Subsequently, cellular lysates were prepared and analyzed for tyrosine phosphorylation of STAT3 by western blot analysis. Figure 6B shows that mIL-6-RFP inhibits IL-6 but not IL-11 and OSM. An about 10-fold surplus of mIL-6-RFP over IL-6 is sufficient to reduce STAT3 phosphorylation to background levels. The same surplus does not inhibit IL-11 activity. Remarkably, even a 110-fold molar surplus of mIL-6-RFP over OSM does not lead to a reduction of STAT3 phosphorylation.

IL-6-mediated biological effects can be transmitted by both membrane-bound and soluble IL-6Rα. The latter process has been termed trans-signaling. The role of trans-signaling in disease progression is considerable because in the presence of soluble IL-6Rα cell populations lacking membrane-bound IL-6Rα gain responsiveness to IL-6 (Scheller et al., 2006). The effect of mIL-6-RFP on IL-6 trans-signaling and on CNTF activity was analyzed on HEK293 cells that express only low amounts of membrane-bound IL-6Rα (Figure 6C). STAT3 phosphorylation in response to IL-6/sIL-6Rα stimulation is completely blocked in the presence of mIL-6-RFP. CNTF-induced STAT3 phosphorylation is unaffected. Similar observations were made with SH-SY5Y neuroblastoma cells (data not shown). mIL-6-RFP not only acts on established cell lines but also on primary cells as is shown by the inhibition of IL-6 activity on primary rat hepatocytes (Figure 6D). Thus, mIL-6-RFP is a highly potent and cytokine-specific inhibitor of IL-6 signaling through membrane-bound and soluble IL-6Rα that exhibits cross-reactivity for human, murine, and rat IL-6.

Comparison of mIL-6-RFP with an IL-6-Neutralizing Monoclonal Antibody

Neutralizing antibodies against a cytokine or its receptor are often used to block cytokine activity. In the following experiment, we compared the inhibitory activities of mIL-6-RFP and a well

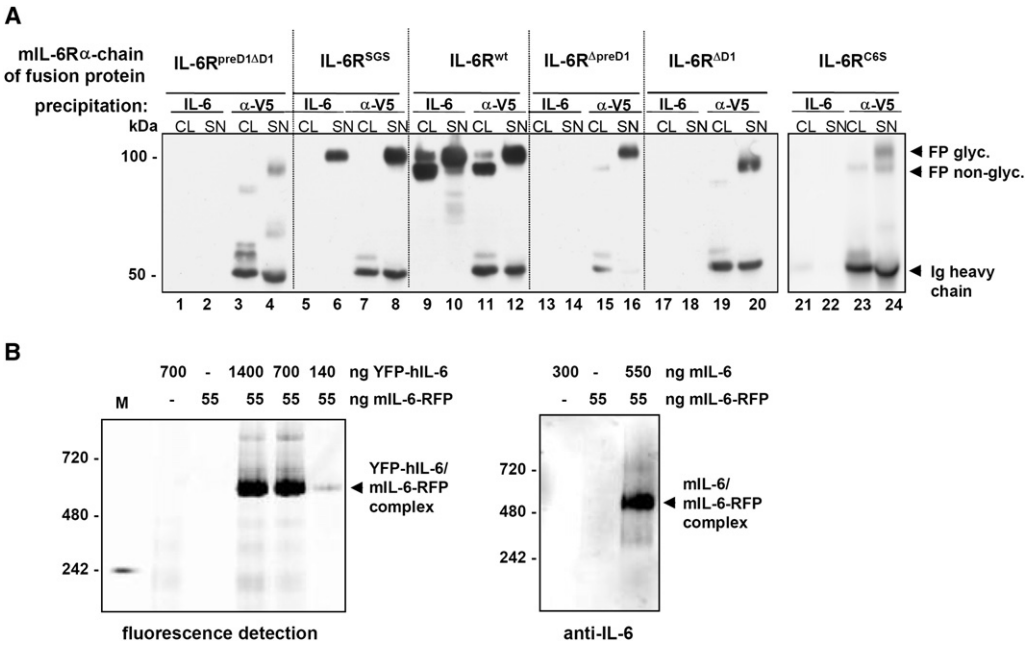

Figure 5. IL-6 Binding of mIL-6Rα Mutants in the Context of a Receptor Fusion Protein

(A) All mIL-6Rα mutants were stably expressed as receptor fusion proteins with a C-terminal V5 epitope tag in HEK293 cells. Fusion proteins were precipitated from cellular lysates (CL) or cell supernatants (SN) by either IL-6 Sepharose or a V5 epitope antibody. Precipitates were analyzed by western blotting using the V5 epitope antibody.

(B) YFP-hIL-6 or mIL-6 were incubated with mIL-6-RFP for 30 min at room temperature. Protein complexes formed were analyzed by native polyacrylamide gel electrophoresis (4%–16% polyacrylamide gradient). The gel loaded with YFP-hIL-6 was analyzed with a Typhoon fluorescence scanner (left panel) the gel loaded with mIL-6 was analyzed by western blotting using the mIL-6 antibody mab406.

characterized IL-6-neutralizing antibody, mab406 (LaSpina et al., 2008), on the IL-6-induced proliferation of murine B9 cells. B9 cells were stimulated with a constant amount of IL-6 in the presence of varying concentrations of mIL-6-RFP (Figure 7A) or the IL-6-neutralizing antibody mab406 (Figure 7B). The IC_{50} for both mIL-6-RFP (apparent molecular mass of 100 kDa) and mab406 (150 kDa) is about 4 ng/ml, corresponding to 40 and 27 pM, respectively. Thus, the inhibitory activity of mIL-6-RFP is comparable with an established IL-6-neutralizing antibody.

DISCUSSION

Soluble receptors have been established as highly specific and potent inhibitors of cytokine action. In first approaches, inhibition of cytokines that signal through homooligomeric receptors has been achieved by dimerization of the corresponding soluble receptors through a Fc tag. The best studied example is the TNF inhibitor Etanercept, a soluble TNFR-Fc fusion protein (Goldenberg, 1999). However, most cytokines signal through heteromeric receptors consisting of two different receptor subunits. In such cases, the inhibitor should contain portions of both receptors to achieve high affinity binding. Inhibitors for IL-1, IL-4, and IL-6 have been generated by fusion of the corresponding soluble receptor proteins to an Fc tag. However, after protein expression, the desired heterodimers have to be separated from the homodimeric byproducts (Economides et al., 2003). We developed another approach based on the inline fusion of cytokine receptors. To limit the size of the resulting receptor fusion protein only the domains of the receptors that are involved in ligand binding were integrated in the construct. Based on this strategy we generated the fusion protein hIL-6-RFP, consisting of domains D1–D3 of human gp130, a flexible peptide linker, and domains D2 and D3 of human IL-6Rα. (Ancey et al., 2003; Metz et al., 2007), and recently a receptor fusion protein for the inhibition of leukemia inhibitory factor (Metz et al., 2008).

For the inhibition of IL-6 in murine disease models, a potent and specific inhibitor for murine IL-6 is highly desirable. However, murine IL-6 does not bind to human IL-6Rα and hence not to hIL-6-RFP. Therefore, we intended to generate a fusion protein consisting of the murine receptor proteins. We found that a murine receptor fusion protein built up in analogy to hIL-6-RFP is not active (Figure 1C) although the main epitopes involved in ligand binding are present. An inspection of the structures of gp130 and IL-6Rα based on the solved structures of the human proteins (Boulanger et al., 2003; Varghese et al., 2002) and molecular models of the murine proteins pointed to a differential role of the Ig-like domain in IL-6Rα function. The main differences were found in the preD1 region, a stretch of 14 amino acids preceding domain D1 that folds back to domain D2, and the corresponding region in D2 that interacts with the preD1 region (Figures 2A and 2B). According to the model, the preD1 region might play a role in positioning of the exposed βC-βD loop (loop L2) of D2 that takes part in ligand binding.

The intramolecular interaction of the preD1 region and D2 involves a disulfide bond between Cys6 in the preD1 region and a cysteine residue in D2 (Cys174 in hIL-6Rα corresponding to Cys171 in mIL-6Rα) that is conserved. Mutants of mIL-6Rα

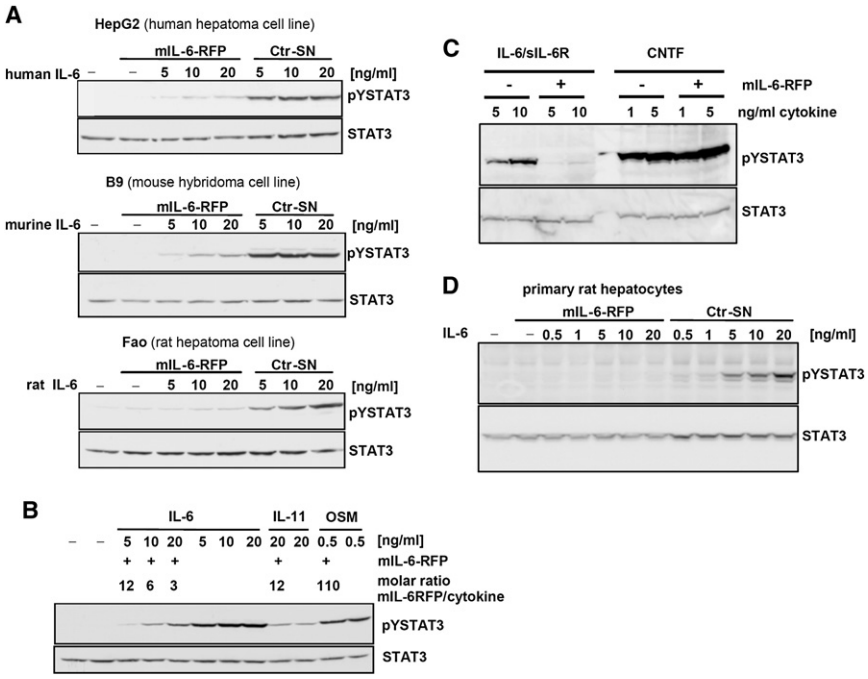

Figure 6. IL-6 Inhibitory Activity of mIL-6-RFP

(A) Concentrated supernatants from HEK293 cells containing 190 ng/ml mIL-6-RFP or concentrated supernatants from mock transfected cells were preincubated for 30 min with the indicated concentrations of human, murine, or rat IL-6 resulting in a 12-, 6-, or 3-fold molar surplus of mIL-6-RFP. The indicated human, murine, and rat cells were stimulated for 20 min. Cellular lysates were analyzed by western blotting. After detection of phosphorylated STAT3 a counterstaining against STAT3 was performed as a loading control.

(B) Concentrated supernatants from stably transfected HEK293 cells containing 190 ng/ml mIL-6-RFP were preincubated with IL-6, IL-11, or OSM at the indicated concentrations for 30 min. HepG2 cells were stimulated for 20 min and cellular lysates were analyzed as described in (A).

(C) Concentrated supernatants from stably transfected HEK293 cells containing 190 ng/ml mIL-6-RFP were preincubated with CNTF or IL-6 (in the presence of 0.5 μg/ml sIL-6Rα) at the indicated concentrations for 30 min. HEK293 cells were stimulated for 20 min and cellular lysates were analyzed as described in (A).

(D) Murine IL-6 at the indicated concentrations was preincubated with supernatants of HEK293 cells containing 190 ng/ml mIL-6-RFP or an equivalent amount of control supernatant for 30 min. Primary rat hepatocytes were stimulated for 20 min and cellular lysates were analyzed as described in (A).

in which this disulfide bond is destroyed (ΔD1, ΔpreD1, and C6S; Figure 2C) are not expressed on the cell surface (Figure 3). In the context of a receptor fusion protein, these mutants are only weakly expressed and devoid of ligand binding activity (Figure 5A). Thus, the disulfide bond is important for protein secretion and receptor function probably by affecting the tertiary structure of D2. Positioning of the preD1 region in front of D2 is not sufficient to restore receptor function, arguing for a synergistic role of D1 and the preD1 region for disulfide bond formation and folding of the domain D2. Deletion of D1, including the preD1 region in the human IL-6Rα, also leads to defective cell surface expression. However, ligand binding is not affected (Vollmer et al., 1999). Therefore, in the context of hIL-6-RFP D2 and D3 of hIL-6Rα are sufficient (Ancey et al., 2003).

Two N-terminal sequence motifs are conserved in IL-6Rα proteins from different species. The hydrophobic LVL motif found in mice, rat, and cattle is replaced by LAP in other species including humans. The larger hydrophobic amino acids of the LVL motif could be involved in a more extensive hydrophobic interaction with D2 that might also be important for positioning of the loop L2. Indeed, replacement of these amino acids by smaller and more hydrophilic residues (SGS mutant; Figure 2C) resulted in a receptor that is less sensitive to stimulation by IL-6 (Figure 4). In the context of the receptor fusion protein, the SGS mutation affects ligand binding (Figure 5A). Thus, the LVL motif might play the proposed role in proper orientation of the L2 loop for IL-6 binding. Even a contribution of the first leucine residue in the site IIIb contact with gp130 is conceivable from the model.

Based on the above structural considerations and the corresponding experimental data, a murine IL-6 receptor fusion protein, mIL-6-RFP, was designed that consists of D1–D3 of murine gp130, a flexible linker, and D1–D3 of murine IL-6Rα including the preD1 region. The molecular mass of the IL-6/IL-6-RFP complex was determined by native gel electrophoresis (Figure 5B). The estimated molecular masses fit to a complex of $(IL\text{-}6)_4(mIL\text{-}6\text{-}RFP)_4$ stoichiometry. According to the X-ray structure of the IL-6 receptor complex (Boulanger et al., 2003), an $(IL\text{-}6)_2(mIL\text{-}6\text{-}RFP)_2$ stoichiometry would have been expected as has been observed for the human IL-6/hIL-6-RFP complex (Metz et al., 2007). The higher order complex formation might be attributed to D1 of IL-6Rα, which is lacking in hIL-6-RFP and in the soluble IL-6Rα used for X-ray crystallography. Higher order receptor complex formation has recently been described for the GM-CSF receptor complex (Hansen et al., 2008).

mIL-6-RFP is a potent inhibitor of murine and rat IL-6. mIL-6-RFP acts through sequestration of the ligand since no IL-6-dependent incorporation of mIL-6-RFP in membrane-bound receptor complexes was detectable (data not shown). It is known that human IL-6 binds to the murine receptors (Grötzinger et al., 1997). Therefore, mIL-6-RFP is also suited for the inhibition of human IL-6 (Figure 6A). Regarding receptor composition, IL-11 is most closely related to IL-6. IL-11 first binds to IL-11Rα that has a similar domain structure as IL-6Rα. Analogous to IL-6, the complex of IL-11 and IL-11Rα signals through a gp130 homodimer (Hilton et al., 1994). OSM signals through a heterodimer of gp130 and the OSM receptor. It has been shown that OSM binds with low affinity to gp130 alone (Staunton et al., 1998).

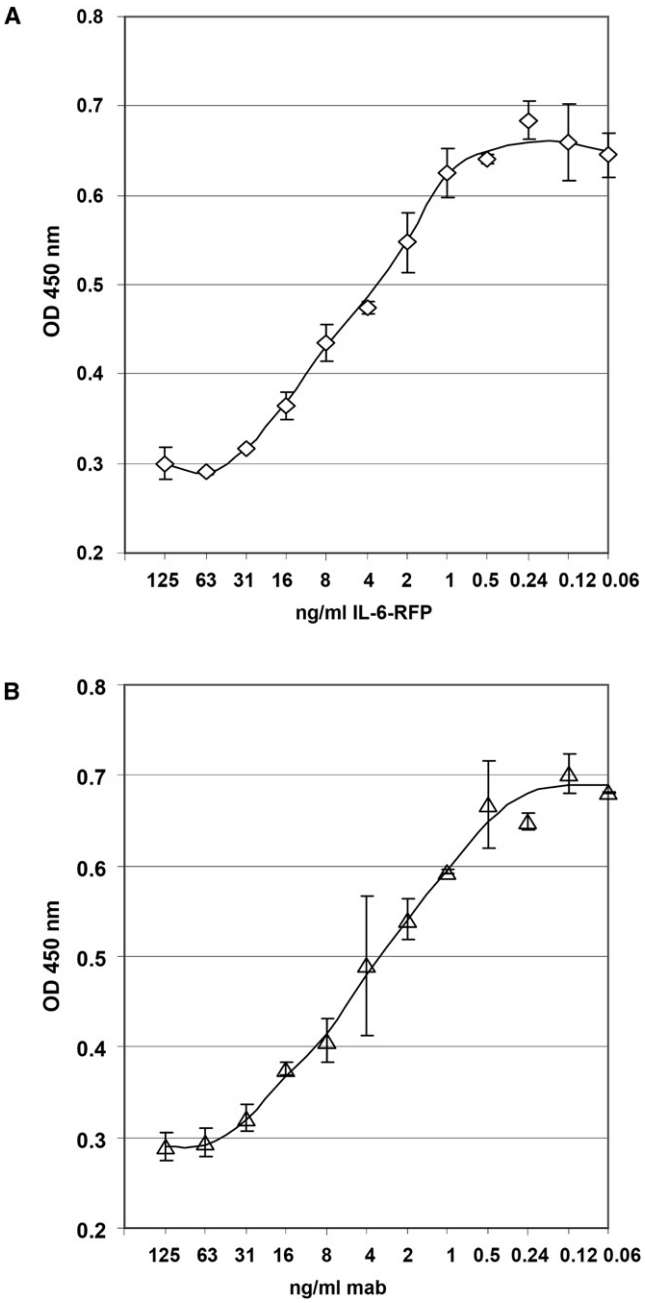

Figure 7. Comparison of the IL-6 Inhibitory Activity of mIL-6-RFP and a Neutralizing IL-6 Antibody

(A and B) B9 cells were incubated with a constant amount of mIL-6 (10 pg/ml) in the presence of mIL-6-RFP or the neutralizing IL-6 antibody (mab406) at different concentrations (serial 2-fold dilutions). After 72 hr of incubation, viable cells were quantified using the colorimetric XTT assay. Mean values from three independent experiments are shown with standard deviations.

Nevertheless, at concentrations sufficient for the inhibition of IL-6 the fusion protein mIL-6-RFP does not affect the bioactivity of IL-11 and OSM despite the fact that these cytokines share the cytokine receptor gp130 with IL-6 (Figure 6B). As human CNTF was reported to bind to human IL-6Rα (Schuster et al., 2003), we tested whether mIL-6-RFP would inhibit CNTF-mediated signaling. However, rat CNTF is not blocked by mIL-6-RFP (Figure 6C), indicating that in rat and murine systems mIL-6-RFP is a specific IL-6 inhibitor.

The complex of IL-6 and soluble IL-6Rα (sIL-6Rα) acts on cells that express gp130 but lack the membrane-bound IL-6Rα. This phenomenon is relevant in certain inflammatory conditions, where IL-6Rα is shed from infiltrating leukocytes by limited proteolysis and sensitizes other cells such as endothelial cells or fibroblast for IL-6 (Scheller et al., 2006). mIL-6-RFP contains the domains D1–D3 of gp130, which are sufficient for binding of IL-6/sIL-6Rα complexes (Horsten et al., 1995). Indeed, mIL-6-RFP blocks IL-6/sIL-6Rα (Figure 6C) irrespective of whether IL-6 and sIL-6Rα have been preincubated or all compounds were added simultaneously (data not shown). Thus, mIL-6-RFP can be regarded as a pan-IL-6 inhibitor that blocks classical as well as trans-signaling.

We found that the inhibitory activity of mIL-6-RFP is comparable to the widely used IL-6-neutralizing monoclonal antibody mab406. If one takes into account that the antibody has two IL-6-binding sites while the fusion protein binds only one IL-6 molecule, the activity per binding site is higher for mIL-6-RFP compared to the antibody. The use of neutralizing monoclonal antibodies in the treatment of IL-6-dependent diseases have been disappointing due to the long half-life of IL-6/antibody complexes (Lu et al., 1992). The accumulation of immune complexes is mediated mainly by the Fc part of the antibody (Vaccaro et al., 2005). Since mIL-6-RFP lacks an Fc fragment it might exhibit more favorable pharmacokinetics that lead to elimination of bound IL-6. Conversely, through the fusion of appropriate protein fragments that increase or diminish the half-life of mIL-6-RFP, the pharmacokinetics might be properly adjusted.

SIGNIFICANCE

In this study we presented the development of a new inhibitor for IL-6, mIL-6-RFP, that was guided by mutagenesis based on a molecular model of mIL-6Rα. In the case of the human receptor fusion protein, the domains directly involved in ligand binding were sufficient. However, for the murine receptor fusion protein, the domain (D1) of mIL-6Rα had to be considered, which is important for the stabilization and adjustment of the neighboring ligand-binding domains (D2 and D3). Thus, for each potential receptor fusion protein the optimal compromise between protein size and structural requirements for function has to be worked out by experimental investigations. The concept of inline fusion of the receptors has the great advantage that the inhibitor is encoded by a single gene, compared to antibodies or cytokine traps where two subunits have to be expressed in parallel. This strategy offers numerous possibilities for specific cytokine inhibition in gene delivery approaches based on viral vectors, transgenic animals, and, finally, gene therapy.

EXPERIMENTAL PROCEDURES

Cytokines and Cytokine Receptors

Recombinant human IL-6 for coupling to CNBr-Sepharose 4B (GE Healthcare) was prepared as described by Arcone et al. (1991). Cytokines used for experiments with cell cultures were purchased from R&D Systems (human and rat

IL-6, human IL-11, and rat CNTF) and PeproTech (murine IL-6 and human OSM). Soluble human IL-6Rα was prepared as described by Weiergräber et al. (1995). His-tagged YFP-IL-6 was expressed in *E. coli* (BL21DE3pLys) and purified by nickel-chelate chromatography on Ni-NTA columns (QIAGEN).

Cell Culture and Transfection of Cells

B9 murine hybridoma cells (DSMZ ACC221) were cultured in RPMI640 (GIBCO) supplemented with 10% FCS (CytoGen) and 50 μM β-mercaptoethanol in the presence of 10–100 pg/ml human IL-6. COS-7 cells (DSMZ ACC60), HEK293 human embryonic kidney cells (DSMZ ACC 305), and FaO rat hepatoma cells (ECACC 89042701) were grown in DMEM (GIBCO) with 10% FCS. HepG2 human hepatoma cells (ATCC HB-8065) were grown in DMEM/F12 (GIBCO) with 10% FCS. Primary rat hepatocytes were prepared as described (Fehrenbach et al., 2001). All cells were cultivated at 37°C in a water-saturated atmosphere containing 5% CO_2. The DEAE-Dextran method and Lipofectamine were used for the transfection of COS-7 cells. HEK293 and HepG2 cells were transfected with Fugene6 (Roche) or Lipofectamine2000 (Invitrogen). Stable transfectants were selected with the antibiotic geneticin (Sigma-Aldrich).

Expression Vectors

The murine IL-6Rα and murine gp130 cDNAs were amplified by RT-PCR using RNA prepared from murine RAW 264.7 macrophages as a template. All expression vectors were constructed using the pcDNA3.1(+) plasmid (Invitrogen). The various constructs encoding the IL-6Rα mutants (Figure 2C) in the context of membrane-bound IL-6Rα-YFP fusion proteins or soluble IL-6 receptor fusion proteins were generated according to standard procedures. The murine IL-6 receptor fusion protein mIL-6-RFP consists of a signal sequence derived from preprotrypsin followed by domains D1, D2, and D3 of mature murine gp130 (up to amino acid arg323), a flexible Ala-Gly-Ser-rich linker of 41 amino acids (Ancey et al., 2003), domains D1, D2, and D3 of mature murine IL-6Rα (up to thr300), and finally a combination of V5 epitope and hexa-histidine tag (V5his tag) for detection.

ELISA

Concentrations of mIL-6-RFP were determined by a sandwich ELISA. A validated antibody combination directed against domains D1–D3 of the mIL-6Rα was used (R&D Systems). Soluble mIL-6Rα (R&D Systems) served as a standard.

Immunoprecipitation, Western Blot, and Native Gels

Recombinant proteins were precipitated either from cell supernatants or lysates of stably transfected cells. Cells in suspension were lysed with radioimmunoprecipitation assay lysis buffer (50 mM Tris-HCl [pH 7.4], 150 mM NaCl, 1 mM EDTA, 0.5% Nonidet P-40, 1 mM NaF, 15% glycerol, 1 mM Na_3VO_4, 1 mM phenylmethylsulfonyl fluoride, 5 μg/ml aprotinin, 5 μg/ml leupeptin, and 3 μg/ml pepstatin A). Other cells were lysed with a Triton-lysis buffer (20 mM HEPES [pH 7.4], 100 mM NaCl, 10 mM β-glycerophosphate, 50 mM NaF, 1% Triton X-100, 1 mM Na_3VO_4, 1 mM phenylmethylsulfonyl fluoride, 5 μg/ml aprotinin, 5 μg/ml leupeptin, and 3 μg/ml pepstatin A). For immunoprecipitations, 5 mg protein A-Sepharose CL-4B (GE Healthcare) preincubated with a mixture of 2.5 μg of each rabbit anti-mouse IgG and either a FLAG (Sigma-Aldrich) or a V5 epitope antibody (Invitrogen). The Sepharose was added to cellular lysates or supernatants for 12 hr. The Sepharose was sedimented by centrifugation and washed with PBS containing 0.05% Tween20 (pH 6.5). The proteins were released by heat treatment in 2× Laemmli buffer and separated by SDS-PAGE. After transfer to a PVDF membrane (Pall Gelman Laboratory) proteins were detected by enhanced chemiluminescence (Pierce) using the respective tag antibody and a horseradish peroxidase-conjugated secondary antibody (DAKO). Proteins precipitated with IL-6-Sepharose were analyzed the same way. STAT3 phosphorylation was detected in cellular lysates by SDS-PAGE and western blotting using a STAT3-pY705 antibody (Cell Signaling). After stripping of the membrane, total STAT3 was stained with a STAT3 antibody (Transduction Laboratories). For native gels, the Novex Bis-Tris gradient gel system (4%–16% polyacrylamide) was used. Gels were run at 4°C. Western blotting of native gels was performed as described in the manual of the supplier (Invitrogen). YFP fluorescence within native gels was detected using a Typhoon fluorescence scanner (Amersham).

Flow Cytometry

Cell surface expression of mIL-6Rα-YFP and the corresponding mutants in the stably transfected HepG2 cells was analyzed by flow cytometry. 2.5×10^6 cells were incubated with a 100-fold diluted mIL-6Rα antibody (anti-CD126; BD Biosciences) and a phycoerythrin-conjugated IgG-$F(ab)_2$ fragment (Dianova). Specificity was controlled using an isotype-matched antibody. Cells (10^5) were analyzed using 488 nm argon laser light for excitation and a 576 nm longpass filter for detection.

EMSA

HepG2 cells stably transfected with mIL-6Rα-YFP wild-type or the SGS mutant were stimulated with different concentrations of mIL-6. Nuclear extracts were prepared as described previously (Andrews and Faller, 1991). Protein concentrations were measured using a NanoDrop spectral photometer (NanoDrop Technologies). A double-stranded mutated sis-inducible element oligonucleotide derived from the c-*fos* promotor (m67SIE [Wagner et al., 1990]: 5′-GATCCGGGAGGGATTTACGGGAAATGCTG-3′) was labeled by filling in 5′-protruding ends with the Klenow enzyme (Roche) using α-[^{32}P]dATP (Hartmann). Nuclear extracts containing 5 mg protein were incubated with 30,000 cpm of labeled oligonucleotide in gel shift incubation buffer (10 mM HEPES [pH 7.8], 1 mM EDTA, 5 mM $MgCl_2$, 10% glycerol, 5 mM DTT, 0.7 mM PMSF, 0.1 mg/ml of poly(dI-dC), and 1 mg/ml BSA) for 10 min at room temperature. The DNA-protein complexes were separated on a 5% polyacrylamide gel containing 7.5% glycerol in 0.25% TBE (200 mM Tris, 166 mM boric acid, and 2 mM EDTA, adjusted to pH 8.3) at 250 V. Gels were fixed in a water solution of 10% methanol and 10% acetic acid for 15 min and dried and autoradiographed using a PhosphoScreen (Kodak) and a Typhoon gel imager (Amersham). Data were analyzed with the program ImageQuant (Molecular Dynamics).

Reporter Gene Assay

HepG2 cells stably transfected with mIL-6Rα-YFP wild-type or the SGS mutant were transiently transfected with a firefly luciferase reporter gene construct under control of the STAT3 inducible rat α2-macroglobulin promoter (pGL3α2M-215-Luc, based on plasmid pGL3 from Promega) and a control plasmid for constitutive expression of renilla luciferase (pGL4.70[hRluc]; Promega). Twelve hours after transfection cells were stimulated for 16 hr with various concentrations of mIL-6. Cells were lysed and luciferase activity was measured with the dual luciferase reporter system (Promega) in a 96 well plate using a luminometer (Berthold).

Proliferation Assay

B9 cells were cultivated in microtest 96 well cell culture plates (Falcon; BD Biosciences) with a constant amount of mIL-6 (10 pg/ml) in the presence of mIL-6-RFP or the neutralizing IL-6 antibody (mab406; R&D Systems) at different concentrations (serial 2-fold dilutions) for 72 hr. Equivalent volumes of mock vector-transfected cell supernatant or isotype-matched IgG were used as controls. After 72 hr of incubation, viable cells were quantified using the Cell Proliferation Kit II (XTT) (Roche).

Confocal Microscopy

Cell surface expression of mIL-6Rα-YFP and the corresponding mutants in the stably transfected HepG2 cells was analyzed by confocal microscopy of living cells using a Zeiss LSM 510 Meta confocal laser scanning microscope and a 63× water-corrected immersion objective with a numerical aperture of 1.2 (C-Apochromat 63×/1.2w). Cells were seeded on 30 mm coverslips and analyzed under cell culture conditions (37°C, 5% CO_2). The membranes of the cells were stained with a 0.5% solution of trypan blue. YFP was excited with laser light of 488 nm and fluorescence was detected using a 505–550 nm bandpass filter. Trypan blue fluorescence was analyzed with the Meta detector above 630 nm. The pinhole was adjusted to 1 Airy unit resulting in optical slices of about 1 μm.

Molecular Modeling

For molecular modeling and graphic representation of protein structures, the programs WHAT IF (Vriend, 1990) and PyMOL (DeLano Scientific) were used. The structure of human IL-6Rα (Varghese et al., 2002) (Brookhaven data bank entry code 1N26) was used as template for the model structure of

murine IL-6Rα. Energy minimizations were performed under vacuum conditions with the GROMOS program library (BIOMOS Biomolecular Software B.V.). The Swiss-Prot accession numbers for the sequences used in the alignment were: mouse, NP_034689; human, BAD97302; pig, BAD97302; rat, P22273; rhesus monkey, XP_001114404; white-tufted ear marmoset, ABH03457; chicken, NP_001038140; dog, XP_855105; cattle, XP_583952.

ACKNOWLEDGMENTS

The authors would like to thank Ralf Weiskirchen for the generous gift of primary rat hepatocytes and Alex Krüttgen for the supply of SH-SY5Y neuroblastoma cells. This work was supported by grants from the Deutsche Forschungsmeinschaft within the Collaborative Research Center SFB 542, projects A2 and Z1 core facility confocal microscopy, and the Fonds der Chemischen Industrie.

Received: October 6, 2008
Revised: May 28, 2009
Accepted: June 24, 2009
Published: July 30, 2009

REFERENCES

Ancey, C., Küster, A., Haan, S., Herrmann, A., Heinrich, P.C., and Müller-Newen, G. (2003). A fusion protein of the gp130 and interleukin-6Ralpha ligand-binding domains acts as a potent interleukin-6 inhibitor. J. Biol. Chem. *278*, 16968–16972.

Andrews, N.C., and Faller, D.V. (1991). A rapid micropreparation technique for extraction of DNA-binding proteins from limiting numbers of mammalian cells. Nucleic Acids Res. *19*, 2499.

Arcone, R., Pucci, P., Zappacosta, F., Fontaine, V., Malorni, A., Marino, G., and Ciliberto, G. (1991). Single-step purification and structural characterization of human interleukin-6 produced in *Escherichia coli* from a T7 RNA polymerase expression vector. Eur. J. Biochem. *198*, 541–547.

Bettelli, E., Korn, T., Oukka, M., and Kuchroo, V.K. (2008). Induction and effector functions of T(H)17 cells. Nature *453*, 1051–1057.

Boulanger, M.J., Chow, D., Brevnova, E.E., and Garcia, K.C. (2003). Hexameric structure and assembly of the interleukin-6/IL-6a-receptor/gp130 complex. Science *300*, 2101–2104.

Economides, A.N., Carpenter, L.R., Rudge, J.S., Wong, V., Koehler-Stec, E.M., Hartnett, C., Pyles, E.A., Xu, X., Daly, T.J., Young, M.R., et al. (2003). Cytokine traps: multi-component, high-affinity blockers of cytokine action. Nat. Med. *9*, 47–52.

Fehrenbach, H., Weiskirchen, R., Kasper, M., and Gressner, A.M. (2001). Up-regulated expression of the receptor for advanced glycation end products in cultured rat hepatic stellate cells during transdifferentiation to myofibroblasts. Hepatology *34*, 943–952.

Goldenberg, M.M. (1999). Etanercept, a novel drug for the treatment of patients with severe, active rheumatoid arthritis. Clin. Ther. *21*, 75–87.

Grötzinger, J., Kurapkat, G., Wollmer, A., Kalai, M., and Rose-John, S. (1997). The family of the IL-6-type cytokines: specificity and promiscuity of the receptor complexes. Proteins *27*, 96–109.

Hansen, G., Hercus, T.R., McClure, B.J., Stomski, F.C., Dottore, M., Powell, J., Ramshaw, H., Woodcock, J.M., Xu, Y., Guthridge, M., et al. (2008). The structure of the GM-CSF receptor complex reveals a distinct mode of cytokine receptor activation. Cell *134*, 496–507.

Heinrich, P.C., Behrmann, I., Haan, S., Hermanns, H.M., Müller-Newen, G., and Schaper, F. (2003). Principles of interleukin (IL)-6-type cytokine signalling and its regulation. Biochem. J. *374*, 1–20.

Hilton, D.J., Hilton, A.A., Raicevic, A., Rakar, S., Harrison-Smith, M., Gough, N.M., Begley, C.G., Metcalf, D., Nicola, N.A., and Willson, T.A. (1994). Cloning of a murine IL-11 receptor alpha-chain; requirement for gp130 for high affinity binding and signal transduction. EMBO J. *13*, 4765–4775.

Horsten, U., Schmitz-Van de Leur, H., Müllberg, J., Heinrich, P.C., and Rose-John, S. (1995). The membrane distal half of gp130 is responsible for the formation of a ternary complex with IL-6 and the IL-6 receptor. FEBS Lett. *360*, 43–46.

Ishihara, K., and Hirano, T. (2002). IL-6 in autoimmune disease and chronic inflammatory proliferative disease. Cytokine Growth Factor Rev. *13*, 357–368.

LaSpina, M., Tripathi, S., Gatto, L.A., Bruch, D., Maier, K.G., and Kittur, D.S. (2008). An interleukin-6-neutralizing antibody prevents cyclosporine-induced nephrotoxicity in mice. J. Surg. Res. *148*, 121–125.

Levine, S.J. (2004). Mechanisms of soluble cytokine receptor generation. J. Immunol. *173*, 5343–5348.

Lu, Z.Y., Brochier, J., Wijdenes, J., Brailly, H., Bataille, R., and Klein, B. (1992). High amounts of circulating interleukin (IL)-6 in the form of monomeric immune complexes during anti-IL-6 therapy. Towards a new methodology for measuring overall cytokine production in human in vivo. Eur. J. Immunol. *22*, 2819–2824.

Metz, S., Wiesinger, M., Vogt, M., Lauks, H., Schmalzing, G., Heinrich, P.C., and Müller-Newen, G. (2007). Characterization of the Interleukin (IL)-6 Inhibitor IL-6-RFP: fused receptor domains act as high affinity cytokine-binding proteins. J. Biol. Chem. *282*, 1238–1248.

Metz, S., Naeth, G., Heinrich, P.C., and Müller-Newen, G. (2008). Novel inhibitors for murine and human leukemia inhibitory factor based on fused soluble receptors. J. Biol. Chem. *283*, 5985–5995.

Müller-Newen, G. (2003). The cytokine receptor gp130: faithfully promiscuous. Sci. STKE *2003*, pe40.

Müller-Newen, G., Küster, A., Hemmann, U., Keul, R., Horsten, U., Martens, A., Graeve, L., Wijdenes, J., and Heinrich, P.C. (1998). Soluble interleukin-6 receptor potentiates the antagonistic activity of soluble gp130 on interleukin-6 responses. J. Immunol. *161*, 6347–6355.

Naugler, W.E., and Karin, M. (2008). The wolf in sheep's clothing: the role of interleukin-6 in immunity, inflammation and cancer. Trends Mol. Med. *14*, 109–119.

Scheller, J., Ohnesorge, N., and Rose-John, S. (2006). Interleukin-6 trans-signalling in chronic inflammation and cancer. Scand. J. Immunol. *63*, 321–329.

Schuster, B., Kovaleva, M., Sun, Y., Regenhard, P., Matthews, V., Grotzinger, J., Rose-John, S., and Kallen, K.J. (2003). Signaling of human ciliary neurotrophic factor (CNTF) revisited. The interleukin-6 receptor can serve as an alpha-receptor for CTNF. J. Biol. Chem. *278*, 9528–9535.

Sepulveda, P., Encabo, A., Carbonell-Uberos, F., and Minana, M.D. (2007). BCL-2 expression is mainly regulated by JAK/STAT3 pathway in human CD34+ hematopoietic cells. Cell Death Differ. *14*, 378–380.

Serada, S., Fujimoto, M., Mihara, M., Koike, N., Ohsugi, Y., Nomura, S., Yoshida, H., Nishikawa, T., Terabe, F., Ohkawara, T., et al. (2008). IL-6 blockade inhibits the induction of myelin antigen-specific Th17 cells and Th1 cells in experimental autoimmune encephalomyelitis. Proc. Natl. Acad. Sci. USA *105*, 9041–9046.

Staunton, D., Hudson, K.R., and Heath, J.K. (1998). The interactions of the cytokine-binding homology region and immunoglobulin-like domains of gp130 with oncostatin M: implications for receptor complex formation. Protein Eng. *11*, 1093–1102.

Vaccaro, C., Zhou, J., Ober, R.J., and Ward, E.S. (2005). Engineering the Fc region of immunoglobulin G to modulate in vivo antibody levels. Nat. Biotechnol. *23*, 1283–1288.

Varghese, J.N., Moritz, R.L., Lou, M.Z., Van Donkelaar, A., Ji, H., Ivancic, N., Branson, K.M., Hall, N.E., and Simpson, R.J. (2002). Structure of the extracellular domains of the human interleukin-6 receptor alpha -chain. Proc. Natl. Acad. Sci. USA *99*, 15959–15964.

Vollmer, P., Oppmann, B., Voltz, N., Fischer, M., and Rose-John, S. (1999). A role for the immunoglobulin-like domain of the human IL-6 receptor. Intracellular protein transport and shedding. Eur. J. Biochem. *263*, 438–446.

Vriend, G. (1990). WHAT IF: a molecular modeling and drug design program. J. Mol. Graph. *8*, 52–56.

 ©2009 Elsevier Ltd All rights reserved

Wagner, B.J., Hayes, T.E., Hoban, C.J., and Cochran, B.H. (1990). The SIF binding element confers sis/PDGF inducibility onto the c-fos promoter. EMBO J. *9*, 4477–4484.

Wegenka, U.M., Lütticken, C., Buschmann, J., Yuan, J., Lottspeich, F., Müller-Esterl, W., Schindler, C., Roeb, E., Heinrich, P.C., and Horn, F. (1994). The interleukin-6-activated acute-phase response factor is antigenically and functionally related to members of the signal transduction and transcription (Stat) factor family. Mol. Cell. Biol. *14*, 3186–3196.

Wei, L.H., Kuo, M.L., Chen, C.A., Chou, C.H., Lai, K.B., Lee, C.N., and Hsieh, C.Y. (2003). Interleukin-6 promotes cervical tumor growth by VEGF-dependent angiogenesis via a STAT3 pathway. Oncogene *22*, 1517–1527.

Weiergräber, O., Hemmann, U., Küster, A., Müller-Newen, G., Schneider, J., Rose-John, S., Kurschat, P., Brakenhoff, J.P., Hart, M.H., Stabel, S., and Heinrich, P.C. (1995). Soluble human interleukin-6 receptor: expression in insect cells, purification and characterization. Eur. J. Biochem. *234*, 661–669.

 ©2009 Elsevier Ltd All rights reserved